Molecular cloning and characterization of presenilin gene in *Bombyx mori*

ZENG-ZHANG ZHENG, MENG-LING CHAO, ZONG-BIAO FAN, YI-JIAO ZHAO and HONG-SHENG SONG

Department of Neurosciences, School of Life Sciences, Shanghai University, Shanghai 200444, P.R. China

Received September 15, 2014; Accepted June 5, 2015

DOI: 10.3892/mmr.2015.4019

Abstract. Presenilin (PS), the catalytic core of the γ-secretase complex, is considered to be a causative protein of the early-onset familial form of Alzheimer's disease. Aging is a risk factor for Alzheimer's disease and a number of genetic studies have utilized *Bombyx mori* (*B. mori*) as a model, making it possible to use *B. mori* to investigate Alzheimer's disease. However, the homologous gene of human *PS* in *B. mori* has remained to be elucidated. In the present study, the *PS* homologue gene in *B. mori* was identified and characterized, and six *B. mori* presenilin (*BmPS*) mRNA transcripts were generated by selecting multiple transcription start sites and/or alternative splice sites. The longest mRNA of *BmPS* (termed *BmPS1*) contains a 153 nt 5' untranslated region (UTR), a 1,440 nt open reading frame and a 1,063 nt 3' UTR. The predicted protein of *BmPS1* consists of 479 amino acid residues and has two highly-conserved aspartate residues, which form the catalytic core of aspartic proteases. It exhibits a sequence identity of ~44 and 51% with homologues in *Homo sapiens* and *Drosophila melanogaster*, respectively. However, the amino acid sequence of the BmPS loop region does not completely match between the two *B. mori* strains R13Q and Dazao. Genomic analysis revealed that *B. mori* had a single copy of the *BmPS* gene, which was composed of 14 exons. A total of four isoforms of *BmPS* (*BmPS*-A, -B, -C and -D) owing to multiple transcriptional start sites and alternative splice sites were identified. The alternative splicing events occurring in the loop region improved the diversity of the *BmPS* protein and were detectable in all tissues, as determined using reverse transcription quantitative polymerase chain reaction (RT-qPCR). Furthermore, the expression levels of *BmPS* in the brain at different developmental stages were detected using RT-qPCR, and significantly higher expression levels of *BmPS* were found in the adult stage compared with those in the larval and pupal stages. The present study on *BmPS* provided insight into the pathogenesis of Alzheimer's disease and mechanisms of silkworm developmental regulation.

Correspondence to: Professor Hong-Sheng Song, Department of Neurosciences, School of Life Sciences, Shanghai University, 99 Shangda Road, Shanghai 200444, P.R. China
E-mail: hssong@shu.edu.cn

Key words: presenilin, *Bombyx mori*, brain, Alzheimer's disease

Introduction

Alzheimer's disease (AD) is a prototypical age-associated neurodegenerative disorder and is the most common progressive form of dementia. Although the pathogenesis of AD remains to be clarified, missense mutations in three associated genes coding for the proteins amyloid precursor protein (APP) and the presenilins (PSs) have been identified as a causative factor in early-onset familial AD (EOFAD) (1-3). Of note, mutations within the PS gene are the most common cause of EOFAD. PS1 mutations account for 18-50% of EOFAD cases (4), while mutations in PS2 are rare (5). PS1 and PS2 are integral membrane proteins with nine transmembrane domains (TMDs) similar in amino acid composition (65%) and intracellular location (6). Of note, PS1 and PS2 exhibit a different tissue-specific expression pattern in transcription level. *PS1* is uniformly expressed (7), while *PS2* is restricted to the heart, skeletal muscle and pancreas (8).

PS is the catalytic core of the γ-secretase complex, containing nicastrin, PS enhancer 2 and anterior pharynx defective 1 (2,9,10). γ-Secretases cleave various type I transmembrane proteins, primarily APP, the Notch receptor, N-cadherin and E-cadherin, which are associated with AD in vertebrates (11). APP, the most well-known substrate of γ-secretase, generates a 37-49 amino acid peptide termed amyloid-β (Aβ) following cleavage. These peptides, particularly Aβ42, are abundantly released and aggregate into oligomeric structures in the brain of patients with an APP or PS missense mutation, and are considered to be the initiating factors of AD (12). In addition, PS has also been reported to regulate the kinase activity and control tau phosphorylation, which is the causative factor of neurofibrillary tangles in AD and other neurodegenerative disorders (13).

A number of invertebrate model organisms, including *Caenorhabditis* (*C.*) *elegans* and *Drosophila* (*D*) *melanogaster*, have been employed to investigate AD, and have provided insight into AD progression and the function of genes involved (14-17). In *C. elegans* and *D. melanogaster*, homologues of *PSs* have been identified. *Sel-12*, the homologous gene of PS in *C. elegans*, has been confirmed to be involved in the lin-12-mediated cell signaling pathway, which is homologous to the Notch pathway in *D. melanogaster* and vertebrates (18). Accumulating evidence has demonstrated that the Notch receptor is the hydrolytic

substrate of Drosophila presenilin (DPS) in *D. melanogaster*, and overexpression of wild-type DPS or DPS mutations in Drosophila resulted in several phenotypes due to loss-of-function of Notch, including wing margin loss, wing vein thickening and rough eye (19-23), which are considered to be the results of an apoptotic process of the developmental wing and eye discs (24). Although Notch is present in the adult brain and is required for long-term memory in *Drosophila* (25), it remains to be elucidated whether DPS regulates long-term memory via Notch signaling. A DPS-null mutation has been reported to impair learning and memory, which, however, cannot be exclusively attributed to loss-of-function in the Notch pathway (26). In addition, DPS is also required for calcium homeostasis, the disruption of which may lead to cognitive deficits (27-29). Similarly to investigations in invertebrates, Notch has also been confirmed to interact with PSs and APP in mammals (30,31) and the expression of Notch 1 is increased in the brains of patients with AD (32). Thus, the understanding of PS and Notch signaling in AD may aid in the development of novel strategies for the treatment of AD. Molecular and genetic studies of PS homologues in invertebrates may also provide important insight into the pathogenic mechanism of this gene family in mammals.

The silkworm, *Bombyx mori (B. mori)*, is widely used in genetics and molecular biology and has numerous beneficial traits as a model compared with mammals or other insects. In particular, the whole genome of the silkworm has been sequenced, which allows for genetic manipulation, and there are already a number of ongoing research projects that utilize transgenic and genetically modified silkworms (33,34). Of note, a number of previous studies have demonstrated the possibility of applying the results obtained in silkworms to mammals (33,34).

To gain insight into the function of *B. mori* presenilin (BmPS), the present study cloned and characterized the *BmPS* gene and assessed its homology with PS from other species. Furthermore, the expression of *BmPS* in various *B. mori* tissues at the adult and larval/pupal stages was assessed. The present study provided a basis for the understanding of the function of PS, particularly with regards to the development of AD.

Materials and methods

Reagents. The reagents and detection kits used in the present study were as follows: LATaq, ExTaq, T4 Ligase, RNase-free DNase I, pMD18 T-Vector, DL2000 DNA marker, DL5000 DNA marker, 5'-Full RACE kit and 3'-Full RACE kit were purchased from Takara Bio, Inc. (Otsu, Japan); ReverTra Ace® kit, KOD Plus ver.2, 100 bp DNA Marker and SYBR® Green real-time PCR master mix were purchased from Toyobo Co., Ltd. (Osaka, Japan); Agarose gel extraction kit, Plasmid mini preparation kit and PCR clean-up kit were purchased from Axygen (Union City, CA, USA); T7 polymerase and PolyATtract® mRNA isolation system III were purchased from Promega Corporation (Madison, WI, USA); TRIzol reagent was purchased from Invitrogen Life Technologies (Carlsbad, CA, USA). Unless stated otherwise, all other chemicals were purchased from Sigma-Aldrich (St. Louis, MO, USA).

Animal model. The two *B. mori* strains, Dazao and R13Q, were kindly provided by Professor Mu-wang Li and Professor An-yin Xu (Department of Biotechnology, Jiangsu University of Science and Technology, Zhenjiang, China). The larvae were reared on fresh mulberries at 25˚C under a 12 h-light/dark cycle. Eggs, pupae and adults were maintained under the same light and temperature conditions.

RNA extraction and reverse transcription polymerase chain reaction (RT-PCR). Total RNA from various tissues of *B. mori* was extracted with TRIzol reagent. A total of 1 μg total RNA was denatured at 65˚C for 5 min and immediately chilled on ice. First-strand cDNA was synthesized using ReverTra Ace® according to the manufacturer's instructions, with Oligo $(dT)_{20}$ primers. Two specific primers F1 and R1 (as shown in Table I) designed from the flanks of the predicted *BmPS* coding sequence (CDS) present in the expressed sequence tag (EST) sequences (BJ983375, BY936068, CK563766, CK490866, CK488524, CK488055 and CK485294) from the SilkBase (http://silkworm.genomics.org.cn/) were used for amplification of the actual CDS. All PCR procedures were performed using LA Taq with GC buffer (Bio-Rad Laboratories, Inc., Hercules, CA, USA) and consisted of 3 min of denaturation at 94˚C followed by 35 cycles of 30 sec at 94˚C, 30 sec at 58˚C and 80 sec at 72˚C, and a final extension step at 72˚C for 5 min.

The expression of *BmPS* alternative splice sites was investigated by RT-PCR using total RNA extracted from R13Q 3rd- and 5th instar larval tissues with the primers of F4 and R5 (as shown in Table I). All PCRs were performed using KOD Plus with 5% dimethyl sulfoxide and consisted of 2 min of denaturation at 94˚C followed by 28 cycles of 10 sec at 98˚C, 30 sec at 58˚C and 20 sec at 68˚C.

The PCR products were purified by 1% agarose gel electrophoresis, sub-cloned into the pMD18-T vector and sequenced by Shanghai Invitrogen Biotechnology Co., Ltd. (Shanghai, China).

Rapid amplification of cDNA ends (RACE). To clone the full-length cDNA of *BmPS*, 5'- and 3'-RACE was performed using the 5'- and 3'-Full RACE kit according to the manufacturer's instructions. For the 5'-RACE, first-strand cDNA was generated by RT of poly(A)$^+$ RNA from the pupal brains of the R13Q strain using the 5'-cDNA synthesis (CDS) primer provided in the kits. The cDNA was amplified by PCR using gene-specific primers (GSPs) and R2/R3 (as shown in Table I), which were synthesized by Sangon Biotech Co., Ltd. (Shanghai, China). To determine the *BmPS* transcripts with multiple transcription start sites and alternative splice sites, 5'-RACE PCR was performed again with the downstream primer R4 and the nest primer R5. In 3'-RACE, first-strand cDNA was generated using the 3'-CDS primer. The cDNA was amplified by PCR using GSPs and F2/F3 (as shown in Table I). The primers F1-1 and R1-1 were used to assess whether the PCR products of 5' and 3' RACE belonged to a single transcript.

RT-quantitative (q)PCR analysis. The brains of 4th instar larvae, 5th instar larvae, pupae and adults were collected from the R13Q strain. The total extracted RNA was treated with DNase to eliminate potential genomic DNA contamination. The RT was performed using the ReverTra Ace kit according to the manufacturer's instructions and was used in the RT-qPCR (iQ5; Bio-Rad Laboratories, Inc.) assays. The negative controls without the RT enzyme were prepared and analyzed in parallel with the unknown samples during the

RT-qPCR assay. RT-qPCR was performed in a 20-μl volume using SYBR Green real-time PCR master mix and the CFX96 system (Bio-Rad Laboratories, Inc.) with template cDNA equivalent to 200 ng RNA and 0.4-mM primers. The primer sequences for *BmPS* are shown in Table I, and the primers for the *BmActin3* gene, as the endogenous control, were as follows: Forward, 5'-GCGCGGCTACTCGTTCACTACC-3' and reverse, 5'-GGATGTCCACGTCGCACTTCA-3'. The two-step amplification protocol consisted of 3 min at 95˚C followed by target amplification via 40 cycles at 95˚C for 15 sec, 63.5˚C for 30 sec and 72˚C for 30 sec. The standard curves were generated by a 10-fold serial dilution of template cDNA, and the reaction efficiency (*E*) was determined by the equation $E=10^{(-1/slope)}$. Quantification analyses of *BmPS* transcript expression relative to *BmActin3* were calculated according to the $2^{-\Delta\Delta Ct}$ method using the CFX Manager software (version 1.6; Bio-Rad Laboratories, Inc.). Data from triplicate experiments are expressed as the mean ± standard deviation.

Sequence analysis. To analyze the intron/exon of the *BmPS*, the *BmPS* sequences were compared with silkworm genomic sequences from the National Center for Biotechnology Information (NCBI) GenBank database (http://www.ncbi.nlm.nih.gov/). The amino acid sequences of *PS* homologues from various species were also retrieved from the GenBank database using the basic local alignment search tool (http://blast.ncbi.nlm.nih.gov/Blast.cgi). Multiple sequence alignments were performed using the DNAman, and phylogenetic analysis was performed with MEGA software, version 5 (http://www.megasoftware.net/).

Statistical analysis of data. Student's one-tailed unpaired t-test was used to perform statistical analysis. A minimum of three independent replicates were used for each treatment and the error bars represent the mean ± standard error.

Results

Cloning of the BmPS gene and its variants. To characterize the *B. mori* presenilin gene (*BmPS*), *BmPS* was cloned from 5th instar larval brains of the R13Q strain. A 1,460-bp fragment (designated BmC-1) was PCR-amplified using the specific primers F1 and R1 (as shown in Table I), which were designed from a conserved amino acid fragment of PSs from the silkworm EST database. Based on the sequence of the original BmC-1 clone, primers were designed for 5'- and 3'-RACE. A total of three fragments (394 bp, 345 bp and 195 bp) were amplified by 5'-RACE with the primer R2 and the nest primer R3 (as shown in Table I). Analysis of the sequence of three fragments indicated that the 5'-region of the *BmPS* transcripts contained at least three transcription start sites and upstream open reading frames (uORFs; Figs. 1 and 2). Only a 1,113-bp fragment was determined by 3'-RACE using the F2 and F3 primers (as shown in Table I and Fig. 2), which exhibited a putative polyadenylation signal (AATAAA) starting 15 nucleotides upstream of the polyA tail (Fig. 1).

To confirm that 5'-RACE, BmC-1 and 3'-RACE belong to the same transcript, the PCR amplification with primers F1-1 and R1-1 (as shown in Table I and Fig. 2) designed from the 5'-UTR and 3'-UTR of *BmPS*s was performed. Only one fragment was obtained and sequence analysis indicated that the PCR products of 5'-RACE, BmC-1 and 3'-RACE belonged to the same transcript. In addition, a novel transcript was identified which had a 33 bp-deletion due to the alternative splicing (Fig. 1).

Table I. Primer sequences designed for *Bombyx mori* presenilin cloning.

Primer	Primer sequence (5'-3')	Position[a]
F1	AGTGACTTAGACGCAACCGAGCA	Exon1
R1	GACTTCTATCTACCTTACGCACA	Exon10
F1-1	TTTGACTTTTATGGTTTTACC	Exon1
R1-1	TTAGTTACGATTCGAATTTG	Exon10
R2	GCTGGAACTCGAGGTTGCTGGG	Exon2
R3	CCCCGATGGGCCACCTTCA	Exon2
R4	CACCTAGACCAAGTTTTACGCCT	Exon9
R5	ACCTTCGCCCTCGACAGTTC	Exon8
F2	ATTTGCGGACGCTTTGGC	Exon10
F3	GAACAGGTGTTCATTTAGC	Exon10
F4	AACGCAATGAGCCTATATTTCCA	Exon5
F5	ATGGACGGCCACATCGCAGAA	Exon1

[a]Positions correspond to Fig. 2. F, forward; R, reverse.

To determine the *BmPS* transcript combinations with multiple transcription start sites and the 33 bp of alternative splicing, 5'-RACE PCR was performed again with primers R4/R5, which are downstream of the 33-bp deletion. The two bands were amplified and sequence analysis of the 30 clones revealed that the *BmPS* gene had six transcripts termed *BmPS1* (2,656 bp), *BmPS2* (2,646 bp), *BmPS3* (2,630 bp), *BmPS4* (2,597 bp), *BmPS5* (2,480 bp) and *BmPS6* (2,447 bp), respectively (Fig. 2). The nucleotide sequences of *BmPS1* and *BmPS2* have been submitted to the GenBank/NCBI database with the accession numbers JQ993471.1 and JQ993472.1, respectively.

Compared with the silkworm genome, *BmPS* was a single gene in *B. mori* and there were at least six splice variants, which were composed of 14 exons (Fig. 2A). In all the alternative splice variants, the introns were in accordance with the GT-AG boundaries rule (data not shown). *BmPS1* (2,656 bp) was the longest transcript, which comprised 13 exons (exon 2-14) and contained a 153 nt 5'-UTR, a 1,440 nt ORF encoding a putative protein of 479 amino acids and a 1,063 nt 3'-UTR (Fig. 1). In addition, three uORFs were identified in the 5'UTRs of BmPS1-6. Among them, BmPS1 possessed uORF1 and uORF3, BmPS2/3/4 possessed uORF2 and uORF3 and BmPS5/6 did not possess any uORFs (Figs. 1 and 2B). The alternative splicing forms of BmPS2/4/6 has a 33 bp deletion (Fig. 2C).

Sequence alignment and phylogenetic analysis. The six transcripts encoded four BmPS isoforms, termed *BmPS*-A (*BmPS1*/*3*), *BmPS*-B (*BmPS2*/*4*), *BmPS*-C (*BmPS5*) and *BmPS*-D (*BmPS6*), which consisted of 479, 468, 463 and 452 amino acid residues, respectively. Alignment of the amino

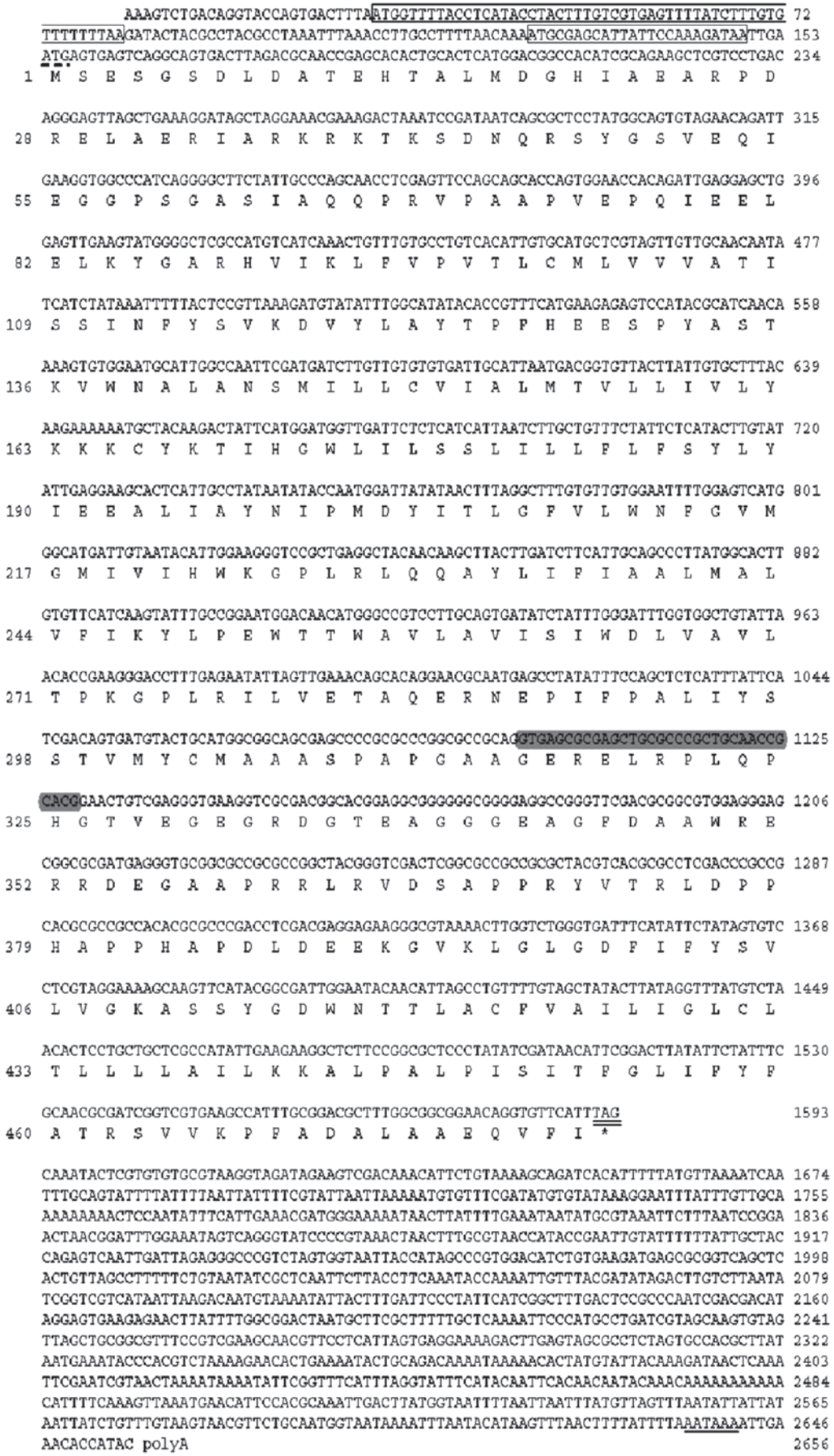

Figure 1. Full-length nucleotide and deduced amino acid sequences of the *BmPS* gene. Numbers on the right refer to the last nucleotide in each line in the corresponding line. The start codon (ATG), stop codon (TAG), and the polyadenylation signal are indicated by a broken underline, double underline and bold underline, respectively. The deduced amino acid sequence is stated below the nucleotide sequence and is numbered to the left. The upstream open reading frames are indicated by a hollow box. The alternative splicing area is shaded. *BmPS*, *Bombyx mori* presenilin.

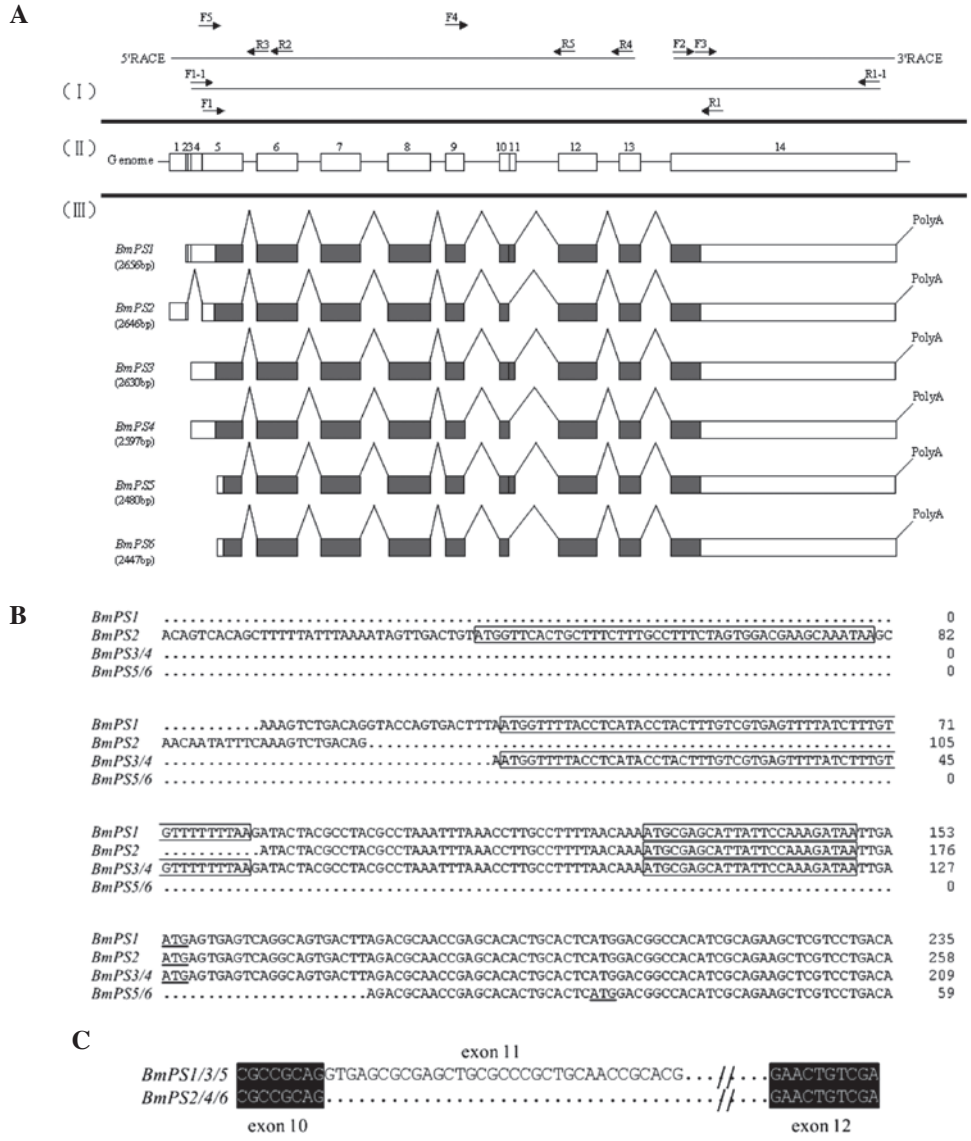

Figure 2. *BmPS* gene structure and splice variants. (A) (I): Primers for the polymerase chain reaction for *BmPS* cloning. Arrows indicate the position and direction of primers. A (II): Genomic organization of the *BmPS* gene. Exons and introns are indicated by white boxes and lines, respectively. A (III): Diagram of the *BmPS* splice variants. Coding regions are indicated by black boxes, non-coding regions by white boxes. Introns are indicated by disconnected lines. ATG: translation initiation; TAG: translation termination. (B) Multiple transcription start sites of *BmPS* transcripts. The upstream open reading frames and translation initiation sites are indicated by hollow boxes and underlines, respectively. (C) The nucleotide sequence spliced region of the *BmPS* transcripts in exon 11. Identical nucleotide residues of exon 10 and exon 12 are highlighted in black. *BmPS*, *Bombix mori* presenilin; RACE, rapid amplification of cDNA ends; F, forward; R, reverse.

acid sequences of the BmPSs with those from mammals and insects indicated a high level of conservation (Fig. 3A). BmPS-A exhibited ~44% sequence identity to hPS1 and hPS2, ~51% to DPS and ~40% to sel-12. In the TMDs, BmPS shared sequence identities of 70% with the human PSs, including the two catalytic aspartate residues (Fig. 3A). Due to the sequence identities in the functional regions of the PS proteins, it was hypothesized that the BmPSs belong to the PS family. In addition, similarly to DPS, one of the BmPS alternative splicing events occurs in the loop region, which is located between TMD6 and TMD7 and had a markedly low level of conservation between species (Fig. 3A). The primers BmPS F1 and BmPS R1 were used to amplify the BmPS in the brains of the Dazao strain, and it was found that there was a 3-amino acid residue insertion in the loop region compared with the R13Q strain (Fig. 3A).

A phylogenetic tree was constructed to analyze the evolutionary associations of BmPS with PSs found in other insects, nematodes, amphibians, reptiles, avian and mammalian/primate species (Fig. 3B). The clustering pattern confirmed that BmPS was grouped in the lineage of other insects (red flour beetle, honey bee, fruit fly and mosquito), with a high bootstrap value, the highest similarity with the PS of *Tribolium castaneum*, whereas avian species (chicken), amphibians (frog), teleosts (zebrafish) and mammals (human and rat) grouped into distinct lineages.

Expression patterns of the B. mori PS gene. In order to determine whether the alternative splicing event in the loop region exhibited tissue-specific expression, the RT-PCR experiments with primers F4 and R5, detecting exon 11 in the ORF, were examined in different tissues of 5th instar silkworm larvae.

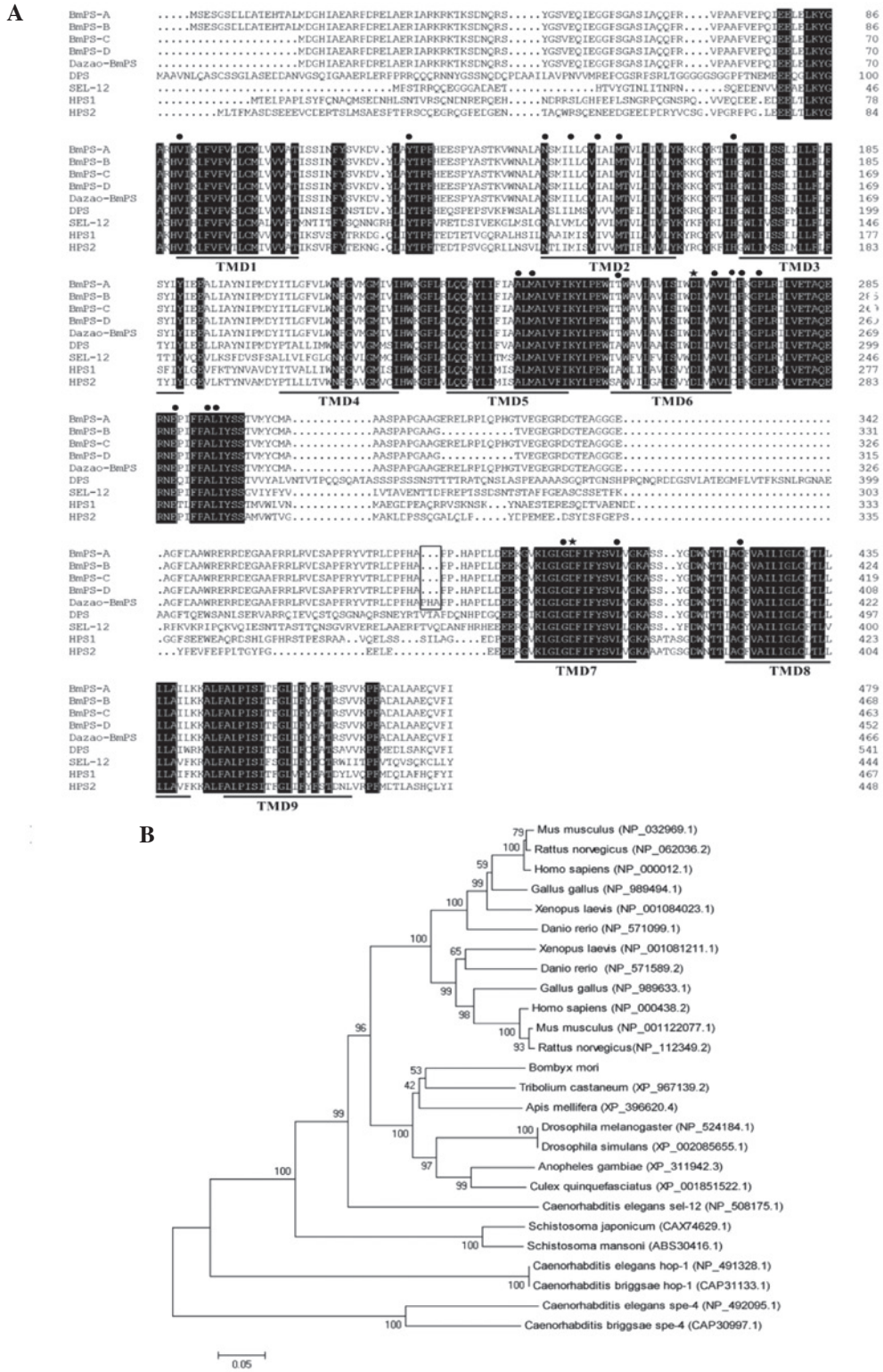

Figure 3. Amino acid sequence alignments and phylogenetic analysis of *BmPS*s and their homologues. (A) Full-length amino acid sequence comparison of PSs from *Bombyx mori* (*BmPS*-A, *BmPS*-B, *BmPS*-C and *BmPS*-D were from the R13Q strain, and Dazao-*BmPS* was from the Dazao strain), *Homo sapiens* [accession nos. NP_000012.1 (hPS1) and NP_000483.2 (hPS2)], *Drosophila melanogaster* [accession no. NP_524184.1 (DPS)] and *Caenorhabditis elegans* [accession no. NP_508175.1 (sel-12)]. Identical amino acid residues are indicated in black. The hPSs transmembrane domains are marked by a single line and the two conserved catalytic aspartate residues and 20 amino acid residues of hPS1/hPS2 mutated in patients with familial Alzheimer's disease are indicated by stars and dots, respectively. The difference in amino acid sequences in *BmPS* between strains R13Q and Dazao is indicated by a hollow box. (B) Phylogenetic tree of PSs, in addition to the species presented in A, of *Tribolium castaneum* (accession no. XP_967139.2), *Apis mellifera* (accession no. XP_396620.4), *Drosophila simulans* (accession no. XP_002085655.1), *Anopheles gambiae* (accession no. XP_311942.3), *Culex quinquefasciatus* (accession no. XP_001851522.1), *Mus musculus* (accession nos. NP_032969.1 and NP_001122077.1), *Rattus norvegicus* (accession nos. NP_062036.2 and NP_112349.2), *Gallus gallus* (accession nos. NP_989494.1 and NP_989633.1), *Xenopus laevis* (accession nos. NP_00104023.1 and NP_001081211.1), *Danio rerio* (accession nos. NP_571099.1 and NP_571589.2), *Caenorhabditis elegans* (accession nos. NP_508175.1, NP_491328.1, CAP31133.1, NP_492095.1 and CAP30997.1), *Schistosoma japonicum* (accession no. CAX74629.1) and *Schistosoma mansoni* (accession no. ABS30416.1). The length of each branch represents the distance between each protein and the common ancestor of that protein and its neighbor. The phylogenic tree was constructed using MEGA5.0 software and the neighbor-joining method. *BmPS*, *Bombyx mori* presenilin. PS, presenilin; TMD, transmembrane domain.

The two bands corresponding to the alternative splicing of *BmPS1/3/5* and *BmPS2/4/6* were detected in the silkworm tissues. The expression of *BmPS2/4/6* was more abundant than that of *BmPS1/3/5*; however, the ratio of *BmPS1/3/5* to *BmPS2/4/6* was 2.2-2.4 in the brain, fat body, silk gland and testes, and 2.7-3.0 in the prothoracic gland, the midgut, malpighian tubules and the ovaries (Fig. 4). This result indicated that *BmPS* and its alternative splicing are expressed in all of the tissues assessed in the present study.

As PS is important in neurodegenerative disorders in mammals and the developmental processes in *Drosophila*, the temporal expression of *BmPS* in the brain was investigated in the present study using RT-qPCR from the larval, pupal and adult stages (Fig. 5). The expression levels of *BmPS* were constant in the 4th instar and the initial stage of the 5th instar, and slowly declined between day 0 of the 5th instar and day 0 of the pupal stage. However, during the development of the pupal stage, the *BmPS* expression levels persistently increased and suddenly markedly improved in the adult stage. This dynamic expression pattern in the brain suggested that *BmPS* may have roles during *B. mori* development, particularly in the adult stages.

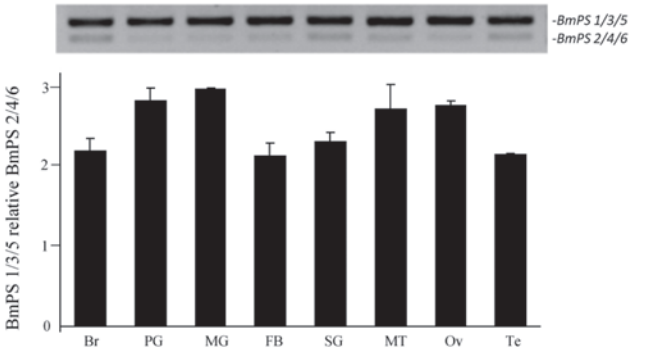

Figure 4. RT-PCR analysis of *BmPS* splice variants in tissues of 3rd- and 5th-day instar larvae of *Bombyx mori* (R13Q strain). *BmPS1/3/5* and *BmPS2/4/6* were detected in the Br, PG, MG, FB, SG, MT, Ov and Te, and the quantification of the RT-PCR results produced by gel imaging system is shown. Data are presented as the mean ± standard error; 3 independent experiments. L, larval; P, pupal; A, adult; *BmPS*, *Bombyx mori* presenilin; RT-PCR, reverse transcription quantitative polymerase chain reaction; Br, brain; PG, prothoracic gland; MG, midgut; FB, fat body; SG, silk gland; MT, malpighian tubules; Ov, ovaries; TE, testis.

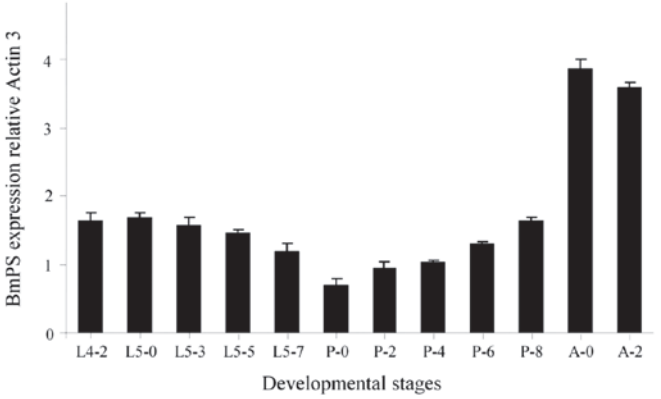

Figure 5. Temporal expression pattern of *BmPS* investigated by reverse transcription-quantitative polymerase chain reaction in the brains of *Bombyx mori* (Dazao strain) developmental stages. L4, L5, P and A present fourth larval instar, fifth larval instar, pupal and adult development, respectively. Numbers in each stage refer to the day in the corresponding developmental stage. Total RNA was extracted from the brain. Expression levels were normalized to the expression of the silkworm Actin 3 gene. Each point represents the mean values of three experiments and error bars indicate the standard error. L, larval; P, pupal; A, adult; *BmPS*, *Bombyx mori* presenilin.

Discussion

PSs are highly conserved transmembrane proteins, which are aspartyl proteases with catalytic residues localized inside the lipid bilayer on TMD6 and TMD7 (2). There are several motifs conserved evolutionarily across numerous species in the two amino acid sequences. The most important motifs include YD and GxGD motifs, which contain catalytic aspartyl residues or an endoplasmic reticulum-retention sequence (35-37). The topology of PSs has established a view of PS as containing nine TMDs (38-40). In metazoans, PS is synthesized as a holoprotein and subsequently undergoes autocatalytic endoproteolysis between TMD6 and TMD7. The conserved two catalytic aspartate residues (Asp^{257} in TM6 and Asp^{385} in TM7 of hPS1) are essential for the released amino- and carboxy-terminal fragments (NTF and CTF, respectively), which are associated with conformational changes in the complex and function together as a heterodimer (41-43). In the present study, a *B. mori* homologue of the PS gene was cloned and characterized. The deduced amino acid sequence of BmPS is equally homologous to DPS (~51% sequence identity), hPS1/hPS2 (~44% sequence identity), the highest similarity with insect PS, particularly *T. castaneum* PS. A total of nine TMDs and the hydrophilic domains at the beginning of the TM6-TM7 loop domain exhibited >70% identity to DPS and hPSs. Two highly-conserved aspartate residues of PS, Asp^{257} in TM6 and Asp^{385} in TM7 of hPS1, corresponded to Asp^{265} and Asp^{397} in BmPS-A. Furthermore, the mutations in hPS1/hPS2, present in human familial AD, have been reported (for a list of the mutations, see molgen.ua.ac.be/ADMutations) (4,44,45). Of note, among the 20 amino acid residues of hPS1/hPS2 mutated in patients with familial AD, 17 are identical and three represent conserved substitutions in BmPS, indicating that the conserved mutations may be important for functions and/or structures of PS. This result suggested that the BmPS cloned in the present study is a member of the PS family and may be relevant to the pathogenesis of AD.

Human PSs have two homologues, hPS1 and hPS2, encoded by two genes on chromsome 14 and chromosome 1, respectively. However, invertebrate PSs, such as *Drosophila* PS, derived from a single gene, exhibit several splice variants (46,47). In *B. mori*, PS has at least six alternative splice sites corresponding to four isoforms, which belong to a single gene. Of note, three uORFs were identified in the 5'-UTR of *BmPS*. uORFs in the 5'-UTR of an mRNA transcript are able to modulate the translational efficiency of the major ORF (mORF), and disruptions of a functional uORF are associated with human genetic diseases (48-51). In *Drosophila*, ~40% of transcripts contain uORFs (52). *DPS* genes also have three uORFs in the 5'-UTR of mRNA (data from FlyBase http://flybase.org/). An upstream ORF has been observed to be involved in Sex lethal to inhibit *msl-2* translation during *Drosophila* gender determination (53). Although

uORF-mediated translational control has been rarely reported in *Bombyx mori*, the translational efficiency of the mORF of *BmPS* may be modulated by the uORFs, highlighting the potential physiological implications of BmPS.

Although PSs share extensive homology throughout their length, the N-terminal domain and the large hydrophilic loop facing the cytosolic compartment between TM6 and TM7 are highly divergent between PS1 and PS2, and are poorly conserved across species. However, numerous PS-linked mutations have been mapped to specific amino acid residues within the loop region, which are highly conserved between species (54,55), the filamin (an actin-binding protein) and the methyltransferases (an evolutionary conserved protein in a variety of species) in *Drosophlia* interact with the loop region of either human or *Drosophila* PSs (56,57), suggesting the functional importance of the loop. Analyzing the BmPS splice variants, the alternative splicing occurs only in the large hydrophilic loop region between TMD6 and TMD7, as exon 11. Similarly, the alternative splice variants of DPS predominantly occur in this region (58). Of note, comparison of BmPS between two silkworm strains R13Q and Dazao showed that the three amino acid residues were inserted in this region in Dazao. It has been established that the strains R13Q and Dazao exhibit morphological and physiological differences, including body stripe, size, voltinism and life span. Although it remains to be elucidated whether the alternative splicing in the TM6-TM7 loop of BmPS has an important function, there remains reason to hypothesize that BmPS may be associated with certain physiological processes in *B. mori*.

PS has been implicated in numerous molecular processes, including Notch signaling, the metabolism of β-catenin and calcium homeostasis (2,19,59-62). mRNAs of *PS*s are ubiquitously detected in a number of human and mouse tissues, including the brain, heart, kidney and muscle (63). In *Drosophila*, DPS is expressed at different developmental stages, exhibiting higher levels of expression in adults than larvae, and is predominantly expressed in the central nervous system (46,47,58). In the present study, *BmPS* and its splice variants were observed to be expressed in the silkworm tissues, including the brain, fat body, silk gland, testis, prothoracic gland, midgut, malpighian tubules and ovaries, and the expression of *BmPS* in the developmental brain was higher in the adult stage. This dynamic expression pattern of *BmPS* suggested that it may have multiple roles during *Bombyx* development.

While vertebrate models provide a closer match to humans from an evolutionary perspective, invertebrates, including the nematode worm *C. elegans* and the fruit fly *D. melanogaster*, have been used extensively in transgenic experiments and classical genetic analyses to investigate the function of AD-relevant genes and to analyze the underlying mechanisms of AD (16,17,64). The Notch signaling pathway was initially linked to AD in *C. elegans* and *D. melanogaster*, contributing greatly to the current understanding of the PS-mediated pathogenesis of AD. Although the silkworm *B. mori*, as a model organism, has not been previously utilized in the study of AD, the present study on *B. mori* PSs may provide valuable insight into the mechanisms of silkworm development regulation and the pathogenesis of AD.

Acknowledgements

The authors would like to thank Professor Yong-hua Ji for encouragement and helpful advice on the manuscript. This study was supported by grants from the National Science Foundation of China (grant no. 31172147) and the Shanghai Committee of Science and Technology (grant nos. 10JC14162002 and 10DZ2271800).

References

1. Tanzi RE: A brief history of Alzheimer's disease gene discovery. J Alzheimers Dis (33 Suppl 1): S5-S13, 2013.
2. Zhang S, Zhang M, Cai F and Song W: Biological function of Presenilin and its role in AD pathogenesis. Transl Neurodegener 2: 15, 2013.
3. Guerreiro RJ, Baquero M, Blesa R, Boada M, Bras JM, Bullido MJ, Calado A, Crook R, Ferreira C, Frank A, *et al*: Genetic screening of Alzheimer's disease genes in Iberian and African samples yields novel mutations in presenilins and APP. Neurobiol Aging 31: 725-731, 2010.
4. Theuns J, Del-Favero J, Dermaut B, van Duijn CM, Backhovens H, Van den Broeck MV, Serneels S, Corsmit E, Broeckhoven CV and Cruts M: Genetic variability in the regulatory region of presenilin1 associated with risk for Alzheimer's disease and variable expression. Hum Mol Genet 9: 325-331, 2000.
5. Bekris LM, Yu CE, Bird TD and Tsuang DW: Genetics of Alzheimer disease. J Geriatr Psychiatry Neurol 23: 213-227, 2010.
6. Schon EA and Area-Gomez E: Is Alzheimer's disease a disorder of mitochondria-associated membranes? J Alzheimers Dis (20 Suppl 2): S281-S292, 2010.
7. Sherrington R, Rogaev EI, Liang Y, Rogaeva EA, Levesque G, Ikeda M, Chi H, Lin C, Li G, Holman K, *et al*: Cloning of a gene bearing missense mutations in early onset familial Alzheimer's disease. Nature 375: 754-760, 1995.
8. Rogaev EI, Sherrington R, Rogaeva EA, Levesque G, Ikeda M, Liang Y, Chi H, Lin C, Holman K, Tsuda T, *et al*: Familial Alzheimer's disease in kindreds with missense mutations in a novel gene on chromosome 1 related to the Alzheimer's Disease type 3 gene. Nature 376: 775-778, 1995.
9. Dries DR and Yu G: Assembly, maturation and trafficking of the gamma-secretase complex in Alzheimer's disease. Curr Alzheimer Res 5: 132-146, 2008.
10. De Strooper B: Aph-1, pen-2 and nicastrin with presenilin generate an active gamma-secretase complex. Neuron 38: 9-12, 2003.
11. Bergmans BA and De Strooper B: Gamma-secretases: From cell biology to therapeutic strategies. Lancet Neurol 9: 215-226, 2010.
12. Querfurth HW and LaFerla FM: Alzheimer's Disease. N Engl J Med 362: 329-344, 2010.
13. Baki L, Shioi J, Wen P, Shao Z, Schwarzman A, Gama-Sosa M, Neve R and Robakis NK: PS1 activates PI3K thus inhibiting GSK-3 activity and tau over phosphorylation: effects of FAD mutations. EMBO J 23: 2586-2596, 2004.
14. Mhatre SD, Paddock BE, Saunders AJ and Marenda DR: Invertebrate models of Alzheimer's disease. J Alzheimers Dis 33: 3-16, 2013.
15. Bonner JM and Boulianne GL: Drosophila as a model to study age-related neurodegenerative disorders: Alzheimer's disease. Exp Gerontol 46: 335-339, 2011.
16. Moloney A, Sattelle DB, Lomas DA and Crowther DC: Alzheimer's disease: Insights from Drosophila melanogaster models. Trends Biochem Sci 35: 228-235, 2010.
17. Link CD: Invertebrate models of Alzheimer's disease. Genes Brain Behav 4: 147-156, 2005.
18. Levitan D and Greenwald I: Facilitation of lin-12-mediated signalling by sel-12, a Caenorhabditis elegans S182 Alzheimer's disease gene. Nature 377: 351-354, 1995.
19. Struhl G and Greenwald I: Presenilin is required for activity and nuclear access of notch in Drosophila. Nature 398: 522-525, 1999.
20. Ye YH, Lukinova N and Fortini ME: Neurogenic phenotypes and altered notch processing in Drosophila Presenilin mutants. Nature 398: 525-529, 1999.
21. Guo Y, Livne-Bar I, Zhou L and Boulianne GL: Drosophila presenilin is required for neuronal differentiation and affects notch subcellular localization and signaling. J Neurosci 19: 8435-8442, 1999.

22. Mahoney MB, Parks AL, Ruddy DA, Tiong SY, Esengil H, Phan AC, Philandrinos P, Winter CG, Chatterjee R, Huppert K, *et al*: Presenilin-based genetic screens in *Drosophila melanogaster* identify novel notch pathway modifiers. Genetics 172: 2309-2324, 2006.
23. van de Hoef DL, Hughes J, Livne-Bar I, Garza D, Konsolaki M and Boulianne GL: Identifying genes that interact with *Drosophila presenilin* and amyloid precursor protein. Genesis 47: 246-260, 2009.
24. Ye YH and Fortini ME: Apoptotic activities of wild-type and Alzheimer's disease-related mutant presenilins in *Drosophila melanogaster*. J Cell Biol 146: 1351-1364, 1999.
25. Presente A, Boyles RS, Serway CN, de Belle JS and Andres AJ: Notch is required for long-term memory in *Drosophila*. Proc Natl Acad Sci USA 101: 1764-1768, 2004.
26. Knight D, Iliadi K, Charlton MP, Atwood HL and Boulianne GL: Presynaptic plasticity and associative learning are impaired in a *Drosophila presenilin* null mutant. Dev Neurobiol 67: 1598-1613, 2007.
27. Lu Y, Lv Y, Ye Y, Wang Y, Hong Y, Fortini ME, Zhong Y and Xie Z: A role for presenilin in post-stress regulation: Effects of presenilin mutations on Ca2+ currents in *Drosophila*. FASEB J 21: 2368-2378, 2007.
28. Michno K, Knight D, Campussano JM, van de Hoef D and Boulianne GL: Intracellular calcium deficits in *Drosophila* cholinergic neurons expressing wild type or FAD-mutant presenilin. PLoS One 4: e6904, 2009.
29. McBride SM, Choi CH, Schoenfeld BP, Bell AJ, Liebelt DA, Ferreiro D, Choi RJ, Hinchey P, Kollaros M, Terlizzi AM, *et al*: Pharmacological and genetic reversal of age-dependent cognitive deficits attributable to decreased presenilin function. J Neurosci 30: 9510-9522, 2010.
30. Ray WJ, Yao M, Nowotny P, Mumm J, Zhang WJ, Wu JY, Kopan R and Goate AM: Evidence for a physical interaction between presenilin and Notch. Proc Natl Acad Sci USA 96: 3263-3268, 1999.
31. Roncarati R, Sestan N, Scheinfeld MH, Berechid BE, Lopez PA, Meucci O, McGlade JC, Rakic P and D'Adamio L: The gamma-secretase-generated intracellular domain of beta-amyloid precursor protein binds Numb and inhibits Notch signaling. Proc Natl Acad Sci USA 99: 7102-7107, 2002.
32. Woo HN, Park JS, Gwon AR, Arumugam TV and Jo DG: Alzheimer's disease and notch signaling. Biochem Biophys Res Commun 390: 1093-1097, 2009.
33. Matsumoto Y, Sumiya E, Sugita T and Sekimizu K: An invertebrate hyperglycemic model for the identification of anti-diabetic drugs. PLoS One 6: e18292, 2011.
34. Sekimizu N, Paudel A and Hamamoto H: Animal welfare and use of silkworm as a model animal. Drug Discov Ther 6: 226-229, 2012.
35. Kaether C, Capell A, Edbauer D, Winkler E, Novak B, Steiner H and Haass C: The presenilin C-terminus is required for ER-retention, nicastrin-binding and gamma-secretase activity. EMBO J 23: 4738-4748, 2004.
36. Wolfe MS: Gamma-secretase in biology and medicine. Semin Cell Dev Biol 20: 219-224, 2009.
37. Fassler M, Li X and Kaether C: Polar transmembrane-based amino acids in presenilin 1 are involved in endoplasmic reticulum localization, Pen2 protein binding and γ-secretase complex stabilization. J Biol Chem 286: 38390-38396, 2011.
38. Sato C, Takagi S, Tomita T and Iwatsubo T: The C-terminal PAL motif and transmembrane domain 9 of presenilin 1 are involved in the formation of the catalytic pore of the gamma-secretase. J Neurosci 28: 6264-6271, 2008.
39. Tolia A, Horré K and De Strooper B: Transmembrane domain 9 of presenilin determines the dynamic conformation of the catalytic site of gamma-secretase. J Biol Chem 283: 19793-19803, 2008.
40. Sobhanifar S, Schneider B, Löhr F, Gottstein D, Ikeya T, Mlynarczyk K, Pulawski W, Ghoshdastider U, Kolinski M, Filipek S, *et al*: Structural investigation of the C-terminal catalytic fragment of presenilin 1. Proc Natl Acad Sci USA 107: 9644-9649, 2010.
41. Shirotani K, Edbauer D, Capell A, Schmitz J, Steiner H and Haass C: Gamma-secretase activity is associated with a conformational change of nicastrin. J Biol Chem 278: 16474-16477, 2003.
42. Deng Y, Tarassishin L, Kallhoff V, Peethumnongsin E, Wu L, Li YM and Zheng H: Deletion of presenilin 1 hydrophilic loop sequence leads to impaired gamma-secretase activity and exacerbated amyloid pathology. J Neurosci 26: 3845-3854, 2006.
43. McCarthy JV, Twomey C and Wujek P: Presenilin-dependent regulated intramembrane proteolysis and gamma-secretase activity. Cell Mol Life Sci 66: 1534-1555, 2009.
44. Boteva K, Vitek M, Mitsuda H, de Silva H, Xu PT, Small G and Gilbert JR: Mutation analysis of presenillin 1 gene in Alzheimer's disease. Lancet 347: 130-131, 1996.
45. Chapman J, Asherov A, Wang N, Treves TA, Korczyn AD and Goldfarb LG: Familial Alzheimer's disease associated with S182 codon 286 mutation. Lancet 346: 1040, 1995.
46. Boulianne GL, Livne-Bar I, Humphreys JM, Liang Y, Lin C, Rogaev E and St George-Hyslop P: Cloning and characterization of the *Drosophila presenilin* homologue. Neuroreport 8: 1025-1029, 1997.
47. Hong CS and Koo EH: Isolation and characterization of *Drosophila presenilin* homolog. Neuroreport 8: 665-668. 1997.
48. Calvo SE, Pagliarini DJ and Mootha VK: Upstream open reading frames cause widespread reduction of protein expression and are polymorphic among humans. Proc Natl Acad Sci USA 106: 7507-7512, 2009.
49. Morris DR and Geballe AP: Upstream open reading frames as regulators of mRNA translation. Mol Cell Biol 20: 8635-8642, 2000.
50. Scheper GC, van der Knaap MS and Proud CG: Translation matters: Protein synthesis defects in inherited disease. Nat Rev Genet 8: 711-723, 2007.
51. Wen Y, Liu Y, Xu Y, Zhao Y, Hua R, Wang K, Sun M, Li Y, Yang S, Zhang XJ, *et al*: Loss-of-function mutations of an inhibitory upstream ORF in the human hairless transcript cause Marie Unna hereditary hypotrichosis. Nat Genet 41: 228-233, 2009.
52. Hayden CA and Bosco G: Comparative genomic analysis of novel conserved peptide upstream open reading frames in *Drosophila melanogaster* and other dipteran species. BMC Genomics 9: 61, 2008.
53. Yao P and Fox PL: Sex lethal and upstream ORFs: A bait-and-trap system for ribosomes. Genome Biol 12: 121, 2011.
54. Tolia A, Chávez-Gutiérrez L and De Strooper B: Contribution of presenilin transmembrane domains 6 and 7 to a water-containing cavity in the gamma-secretase complex. J Biol Chem 281: 27633-27642, 2006.
55. Wanngren J, Frånberg J, Svensson AI, Laudon H, Olsson F, Winblad B, Liu F, Näslund J, Lundkvist J and Karlström H: The large hydrophilic loop of presenilin 1 is important for regulating gamma-secretase complex assembly and dictating the amyloid beta peptide (Abeta) Profile without affecting Notch processing. J Biol Chem 285: 8527-8536, 2010.
56. Guo YQ, Zhang SX, Sokol N, Cooley L and Boulianne GL: Physical and genetic interaction of filamin with presenilin in Drosophila. J Cell Sci 113: 3499-3508, 2000.
57. Zhang SX, Gua Y and Boulianne GL: Identification of a novel family of putative methyltransferases that interact with human and *Drosophila* presenilins. Gene 280: 135-144, 2001.
58. Nowotny P, Gorski SM, Han SW, Philips K, Ray WJ, Nowotny V, Jones CJ, Clark RF, Cagan RL and Goate AM: Posttranslational modification and plasma membrane localization of the Drosophila melanogaster presenilin. Mol Cell Neurosci 15: 88-98, 2000.
59. Song W, Nadeau P, Yuan M, Yang X, Shen J and Yankner BA: Proteolytic release and nuclear translocation of Notch-1 are induced by presenilin-1 and impaired by pathogenic presenilin-1 mutations. Proc Natl Acad Sci USA 96: 6959-6963, 1999.
60. Kang DE, Soriano S, Frosch MP, Collins T, Naruse S, Sisodia SS, Leibowitz G, Levine F and Koo EH: Presenilin 1 facilitates the constitutive turnover of β-catenin: Differential activity of Alzheimer's disease-linked PS1 mutants in β-catenin-signaling pathway. J Neurosci 19: 4229-4237, 1999.
61. Stutzmann GE, Caccamo A, LaFerla FM and Parker I: Dysregulated IP3 signaling in cortical neurons of knock-in mice expressing an Alzheimer's-linked mutation in presenilin1 results in exaggerated Ca2+ signals and altered membrane excitability. J Neurosci 24: 508-513, 2004.
62. Soriano S, Kang DE, Fu M, Pestell R, Chevallier N, Zheng H and Koo EH: Presenilin 1 negatively regulates beta-catenin/T cell factor/lymphoid enhancer factor-1 signaling independently of beta-amyloid precursor protein and notch processing. J Cell Biol 152: 785-794, 2001.
63. Lee MK, Slunt HH, Martin LJ, Thinakaran G, Kim G, Gandy SE, Seeger M, Koo E, Price DL and Sisodia SS: Expression of presenilin 1 and 2 (PS1 and PS2) in human and murine tissues. J Neurosci 16: 7513-7525, 1996.
64. Dillin A and Cohen E: Ageing and protein aggregation-mediated disorders: from invertebrates to mammals. Philos Trans R Soc Lond B Biol Sci 366: 94-98, 2011.